Design and Performance of a Digitally Based Voltage Controller for Correcting Phase Unbalance in Induction Machines

JUN OYAMA, MEMBER, IEEE, FRANCESCO PROFUMO, MEMBER, IEEE, EDUARD MULJADI, MEMBER, IEEE, AND THOMAS A. LIPO, FELLOW, IEEE

Abstract—**The case of unbalanced supply presents a uniquely difficult problem in motor application since its causes are varied. In many situations a static starter utilizing back-to-back thyristors in series with the motor lines is already installed for the purpose of soft starting or for power factor improvement. An attractive low-cost solution for phase unbalance is simply to modify the control strategy of the static starter by adjusting the firing angles of the three thyristor pairs independently. In this manner the series connected thyristors serve the function of unsymmetrical, variable supply impedances which can be used to balance the voltage across the motor phases. A new digital controller utilizing a static starter for balancing the phase currents of an induction motor operating with unbalanced supply is presented. Experimental results show a marked reduction in the current unbalance from approximately 40% to a few percent and clearly demonstrate the attractiveness of the new phase balancer.**

Introduction

THE CASE of unbalanced supply presents a uniquely difficult problem in motor application since the causes of such unbalances arise from numerous unsymmetrical conditions. Unsymmetrical transformer windings or transmission line impedance, unbalanced three phase loads or a large single phase load, are some typical examples. Causes exist in all stages of the electrical energy transformation from the generation to utilization. However, regardless of the cause, even a small phase voltage unbalance can induce large negative sequence currents due to the relatively low negative sequence impedance of the connected ac machine. Induction motors are particularly sensitive to unbalanced operation since localized heating can occur in the stator and the life of the machine can be seriously affected with only a few percent voltage unbalance.

Conventional remedies for phase unbalance often involve costly modification of the incoming substation equipment, redesign of the feeder line layout to the various loads, or perhaps, retrofit with an oversized machine. In many situations, however, a static starter utilizing back-to-back thyristors in series with the motor lines is already installed for the purpose of soft starting or for power factor improvement. Hence an attractive low-cost solution for correcting the phase unbalance problem would be simply to modify the control strategy of the static starter by adjusting firing the angles of the three thyristor pairs independently [1]. In this manner the series connected thyristors serve the function of unsymmetrical variable supply impedances which can be used to balance the voltage across the motor phases [2].

A new digital controller utilizing a static starter for balancing the phase currents of an induction motor operating with an unbalanced supply is the topic of this paper. The benefits obtainable by this solution are not only reduction in hot spots inside the machine but also, with drastic reduction of the negative sequence of current and voltage, it is possible to improve also the motor efficiency, to limit the level of the flux saturation inside the machine and also to eliminate acoustic noise and vibration due to torque pulsations.

Approach to Analysis

To avoid the unbalanced voltage problem, a system consisting of three back-to-back thyristors pairs in series with the induction machine phases together with a new control strategy that provides different firing angles for each phase has been proposed [2]. The block diagram of the overall system is shown in Fig. 1. The three phases constituting an unbalanced supply V_{ai}, V_{bi}, V_{ci} are assumed to feed the converter. The induction machine, on the other side of the converter should be supplied by the balanced three-phase voltages V_{ao}, V_{bo}, V_{co}. The unbalanced conditions are counteracted by the controller to produce balanced voltages across the induction machine terminals. Thus the unbalanced parts of the input voltages drop across the silicon-controlled rectifiers (SCR's) can be represented by a variable series reactance that can be established by means of a fundamental component analysis [3]. The voltage drops in each phase are X_aI_a, X_bI_b, and X_cI_c. To illustrate this condition the related phasor diagram is shown in Fig. 2.

Paper IPCSD 89-26, approved by the Industrial Drives Committee of the IEEE Industry Applications Society for presentation at the 1988 Industry Applications Society Annual Meeting, Pittsburgh, PA, October 2-7. Manuscript released for publication July 25, 1989. This work was supported in part by the Wisconsin Electric Machines and Power Electronics Consortium.

J. Oyama was with the University of Wisconsin, Madison, WI. He is now with the Department of Electrical Engineering and Computer Science, Faculty of Engineering, Nagasaki University 1-14 Bunkyo Machi, Nagasaki, 852 Japan.

F. Profumo was with the University of Wisconsin, Madison, WI. He is now with the Dipartimento di Elettrotecnica, Politecnico di Torino, Corso Duca degli Abruzzi, 24, 10129 Torino, Italy.

E. Muljadi was with the University of Wisconsin, Madison, WI. He is now with the Department of Electrical Engineering, California State University-Fresno, Mail Stop 94, Fresno, CA 93740.

T. A. Lipo is with the Department of Electrical and Computer Engineering, University of Wisconsin, 1415 Johnson Drive, Madison, WI 53706-1691.

IEEE Log Number 9034287.

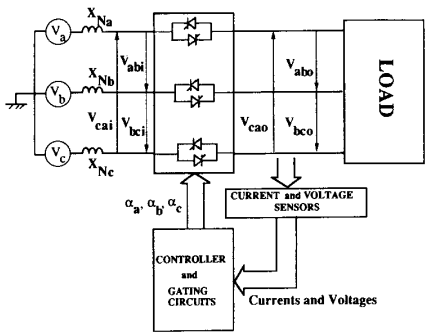

Fig. 1. Block diagram of overall system.

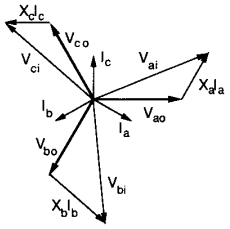

Fig. 2. Phasor diagram of back-to-back thyristor converter.

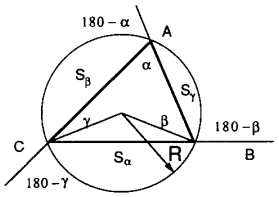

Fig. 3. Triangle plane showing control strategy geometrical analogy.

The main objective of the controller is then to equalize the line current and the losses in each phase. Since losses are proportional to the line current squared, the control variables used are the currents.

In the plane of a triangle ABC, as shown in Fig. 3, the control algorithm can be depicted by a geometrical analogy. The triangle angles are defined as α, β, γ and S_α, S_β, S_γ are the corresponding opposite sides. The relations among the angles and sides for the triangle can be written as follows:

$$\frac{|S_\alpha|}{\sin\alpha} = \frac{|S_\beta|}{\sin\beta} = \frac{|S_\gamma|}{\sin\gamma} = 2R \tag{1}$$

where R is the radius of circumscribed circle.

For any operating condition the following vector equation can be written for the triangle:

$$\vec{S}_\alpha + \vec{S}_\beta + \vec{S}_\gamma = 0. \tag{2}$$

If it is possible to adjust the amplitude of S_α, S_β, S_γ independently and to make them equal, the triangle will then form an equilateral triangle with the following characteristics:

$$|S_\alpha| = |S_\beta| = |S_\gamma| \tag{3}$$

$$\alpha = \beta = \gamma = 60^\circ \tag{4}$$

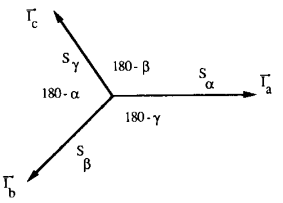

Fig. 4. Asymmetrical currents in triangle plane.

$$R = (|S_\alpha|\sqrt{3})/3. \tag{5}$$

These equations for the triangle can be correlated with a three-phase balanced wye connected induction machine, as shown in Fig. 4. The three-phase line currents for any condition can be written as follows:

$$\vec{I}_a + \vec{I}_b + \vec{I}_c = 0. \tag{6}$$

For balanced conditions, the line currents (in the time domain) are mutually displaced from each other by 120°. By analogy with the triangle, if the amplitude of the three line currents can be maintained equal, the line currents are balanced. Thus, in practice, if the controller maintains the amplitudes of the three line currents equal then, consequently, the phase angles of the three phases are automatically adjusted to their proper values for phase balance as well. This is accomplished through control of the converter by adjusting the firing angles independently on each phase. The "current balancing loops" of Fig. 5 perform this controller function.

In addition, to keep the induction machine operating at the same condition as before the unbalanced condition occurred, the voltage across the phases must be kept constant at the rated condition. In effect, the machine excitation level must be kept constant, and the amplitudes of the balanced currents must return to their original values. This is a further constraint for the system, and it defines the necessary steady-state operating point.

It is useful to consider again the circumscribed circle of Fig. 3. Three conditions might occur during the adjustment of the current amplitudes I_a, I_b, I_c.

a) The radius of the circle is kept constant and equal to R_0. The summation of the line currents amplitudes is the same as before the unbalanced condition occurred.
b) The radius of the circle is larger than the original and equal to R_2. The amplitude of one or more line currents is larger than the original ones.
c) The radius of the circle is smaller than the original and equal to R_1. The amplitude of one or more line currents is smaller than the original ones.

For all three conditions to apply, the controller must be capable of adjusting the three line currents back to its original amplitude. Hence the controller must be able to increase or to decrease the applied voltage to the induction machine terminals. A balanced condition is reached when the circumscribed circle of the line currents return to the original condition (radius equal to R_0). This feature is corresponds to the "voltage loop" in Fig. 5.

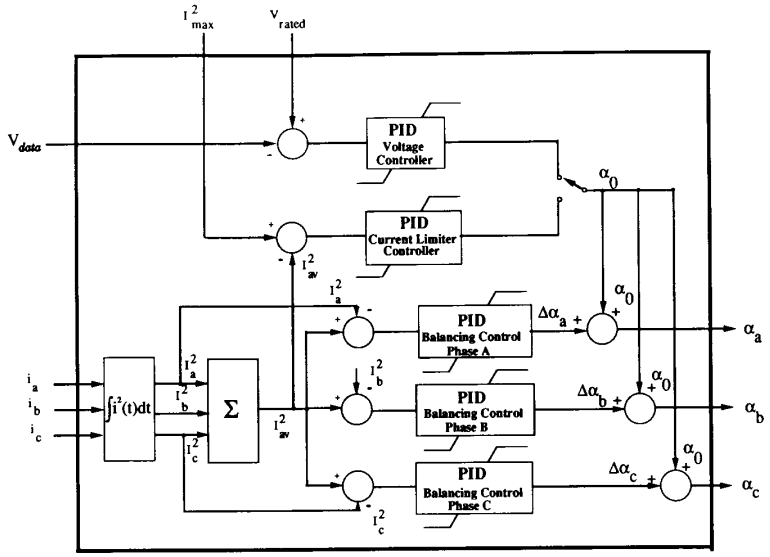

Fig. 5. Control loops block diagram.

Finally, since the nature of the SCR's controller is to adjust the voltage applied to the phases winding by modifying the firing angles, the voltage applied at the induction machine terminals is always smaller than the input voltage of the SCR's converter for any value of firing angle except zero. Therefore, to keep the rated voltage at the terminal input of the induction machine, the incoming voltage to the SCR's converter must be larger than the rated voltage of the induction machine. Thus, under the normal balanced condition, the firing angles must be slightly greater than zero to reduce the incoming voltage (i.e., to match the induction machine voltage). This condition enables the controller not only to reduce but also increase the voltage across the induction machine terminals [1].

Control Strategy

The system proposed in this paper consists of three pairs of identical thyristors, connected back-to-back in series with a three-phase wye (or delta) connected induction machine. In general, the stator voltage control is accomplished by adjusting the holdoff angle γ which corresponds to the time the thyristor remains open after the current reaches zero in a given phase. The aim of the controller is to compensate the unbalanced voltage supply by controlling each pair of thyristor distinctly with an unsymmetrical firing angle such that different values of γ occur in each phase.

Some of the central functions implemented with the digital controller are shown in the block diagram of Fig. 5. The complete control consists of three main loops: a "current limiter loop," a "voltage loop," and finally, a "balancing current loop." Each loop contributes to the calculation of the phase angle α_i separately for each phase with $i = a, b, c$.

The current-limiter loop is a protection control loop and mainly operates during the starting of the machine as well as during overload conditions (transient operations). Such a loop limits the average current in the three phases to the value imposed by the reference value $I_{\max}$. The current limit value can easily set, consistent with the load demands and the connected network characteristics. The voltage loop, on the other hand, is the control loop for the normal balanced condition (steady-state operation). The voltage loop keeps the voltage at the motor terminals at the rated value.

The two previous loops operate alternately rather than simultaneously. The output of either loop contributes to the average phase angle command α_0 which is nominally equal for the three phases. In addition to the voltage and current limiter loops, the balancing current loops, one for each phase, operate both in steady state and during transient conditions and control each phase current to maintain each of them equal to the average value of the three phases. The outputs of the three loops can be different for each phase, related to the unbalanced voltage of each phase and are expressed by the angles: $\Delta\alpha_a$, $\Delta\alpha_b$, $\Delta\alpha_c$. A pictorial representation of the overall phase balancing strategy is shown in Fig. 6. From this figure, the firing angles for the a, b, c phases can be written:

$$\begin{aligned} \alpha_a &= \alpha_0 + \Delta\alpha_a \\ \alpha_b &= \alpha_0 + \Delta\alpha_b \\ \alpha_c &= \alpha_0 + \Delta\alpha_c \end{aligned} \tag{7}$$

where $\Delta\alpha_a$, $\Delta\alpha_b$, $\Delta\alpha_c$ can be positive or negative. For steady-state balanced conditions, the three balancing current loop outputs are equal to zero. This mode of operation can be termed the "voltage mode" because the phase angles are controlled. In addition, a second mode of operation, a so-called "current mode," is possible in which the holdoff angle γ is controlled. Both control schemes have been tested, but the best results have been obtained by the first mode. Hence the results in this paper are always related to the voltage mode.

System Design

To obtain the performances described, the analog controller of a commercial static starter drive has been substituted with

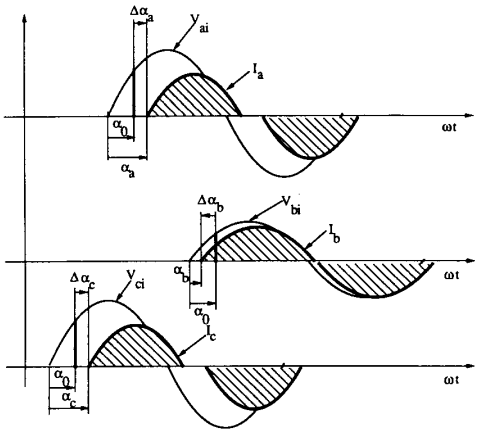

Fig. 6. Current balancing control strategy.

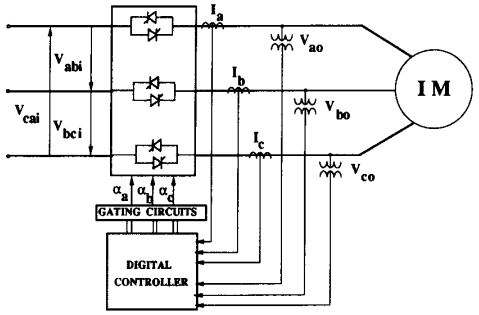

Fig. 7. Overall system with digital controller.

a new digital controller. Fig. 7 shows a simplified block diagram of the overall implementation with the independent firing angles for the three phases, using currents and voltage as feedback signals.

The controller has been implemented digitally in an Intel 8088 low-cost single-board computer. The CPU runs at 5 MHz clock and, as shown in Fig. 8, the board has an 8 kbit EPROM, an 8 kbit RAM, a serial port 8251, interruption controller 8259, parallel I/O controller 8255, and a 8253 counter [4].

In addition, two interface boards have been designed. The first board has a phase-locked loop (PLL) for detecting the system frequency and synchronizing the control functions and a D/A converter for detecting currents or voltages as selected by software. The second board is the I/O board with four A/D converters for the three currents and the voltage feedback and a counter for the gate pulse generator.

The serial interface is the communication link between the single-board computer and the IBM/AT used as a development system. The IBM/AT is also utilized as an input/output terminal for updating the control parameters and checking some control internal variables as the firing angles for each phase. The serial interface was chosen because it is much more robust than other communication interfaces from the noise point of view since it uses the ± 15 V/-15 V as signal level and the parity bit to detect signal errors.

The 8-kbit EPROM is prepared with a basic software that is called a "mini monitor" and mainly consists of a debugger, which is compatible with MS-DOS debugger except for assembly and disassembly commands. In addition, some general use subroutines, particularly beneficial in the stage of the software development, are resident in the EPROM. The 8-kbit RAM is the memory for the applicative software. The software has been written in Assembler language and consists of a main loop and five levels of interruption loops.

The main loop analyzes the keyboard commands and sets and updates the control parameters as the proportional, the derivative and the integral gains for each loop and the references for the voltage loop and for the current limiter loop. In addition, the main loop takes care to store important internal variables: such as currents, voltages, and balancing angles. Finally, the previous variables can be displayed on the screen, selectable by keyboard. Fig. 9 shows a simple flowchart of the main loop.

On the other hand, the interruption loops calculate the rms values for each current and the output of proportional-integral-derivative (PID) control loop. The first level of the interruption loop (INT0) occurs 32 times in each period and calculates I_a^2, I_b^2, and I_c^2. It detects the zero points for the three voltages and in the voltage mode sets the three counters and calculates the PID outputs. Fig. 10 shows a simplified flowchart of the loop INT0 and some details about the integration procedure.

The fifth level of interruption (INT4) occurs once in a cycle and resets the angle counter for the voltage in INT0. Finally INT1–3 occurs once in each semiperiod for each phase, and these signals come from the zero current detectors. In the current mode, they set the three counters, one for each phase and calculate the PID outputs.

Experimental Results

Since the causes of unbalanced supply voltages arise from many sources, it was necessary to decide how the unbalances were to be simulated in our laboratory. A 7.5-hp four-pole 60-Hz 220-V three-phase squirrel-cage induction motor has been utilized, supplied by a static starter which employs six thyristors as its power switching devices. Two different causes of unbalance have been selected and realized. In the first test three voltages with different amplitudes supply the back-to-back thyristor converter. Fig. 11 shows the simplified schematic employing one three-phase autotransformer with an additional single-phase transformer for obtaining the unbalanced voltage. The percentage of unbalanced voltage can be defined by the following expression:

$$V_{\text{unb}} = \frac{V_{abi} - V_{cai}}{V_{cai}} * 100 \tag{8}$$

where the symbols are illustrated in Fig. 11. The second simulation of unbalance has been set by using different line impedance in series with the three phases. Since the results obtained by the two experiments are comparable, the results reported in this paper are related to the first set of experiments.

To evaluate the performance of the prototype, the same mo-

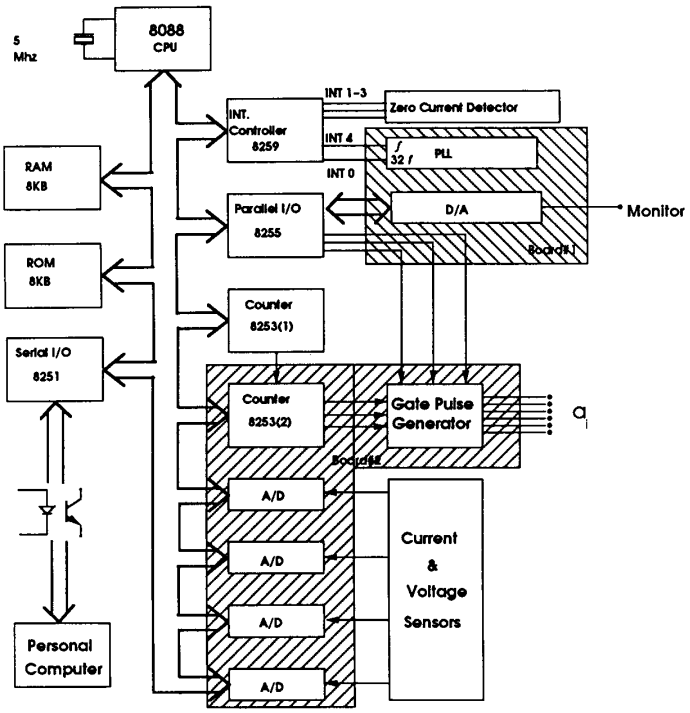

Fig. 8. Hardware configuration of digital controller.

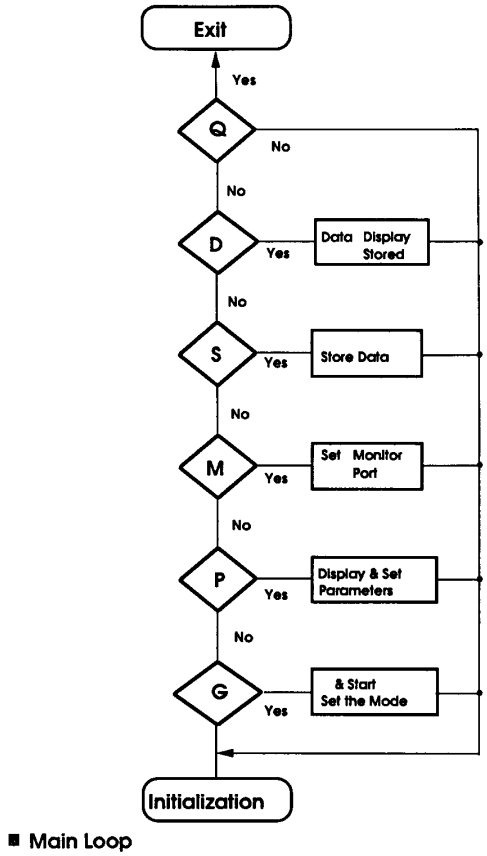

■ Main Loop

Fig. 9. Flowchart of "main loop."

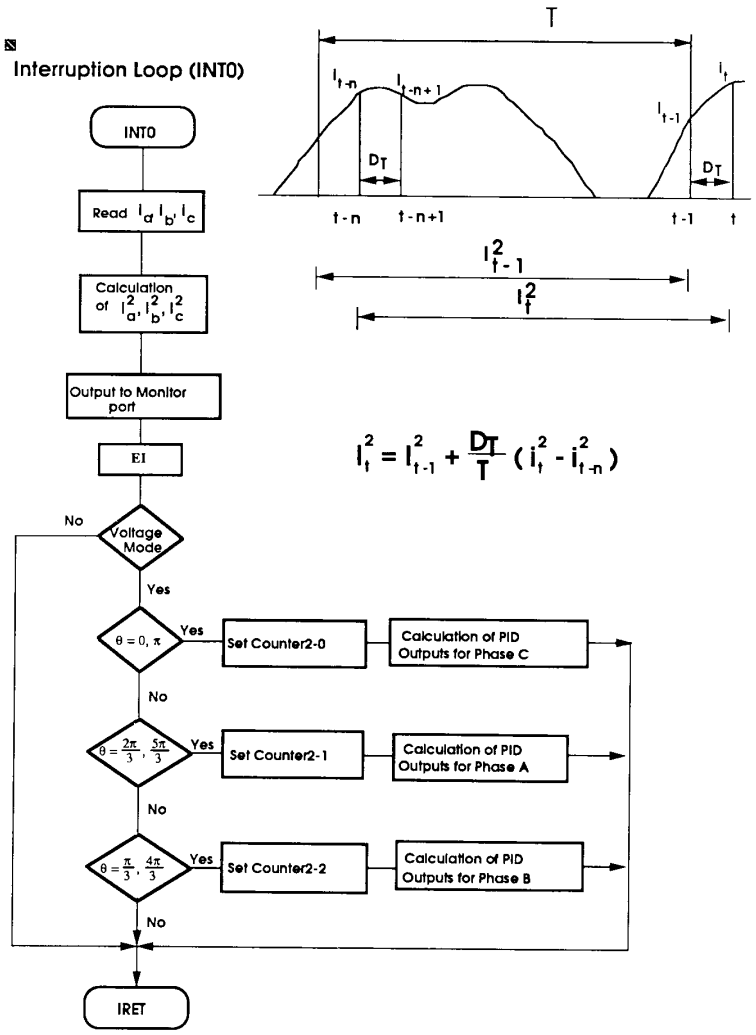

Fig. 10. Flowchart of interruption loop (INT0).

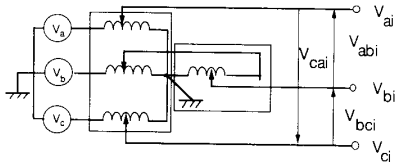

Fig. 11. System for realizing unbalanced power supply.

tor was supplied by two different methods. First, the unbalanced voltage supply mentioned earlier was connected directly to the motor, and different percentages of unbalanced voltage were supplied to the load (EXPER.1). The test has been repeated employing the static starter prototype supplied by the unbalanced voltage supply (EXPER.2).

Fig. 12 shows the currents in phases b and c when the motor is supplied by a sinusoidal waveform (EXPER.1) with $V_{unb} = +8\%$ and when the machine is operating under a full-load condition. It is interesting to note that the currents become nonsinusoidal even for the sinusoidal supply due to

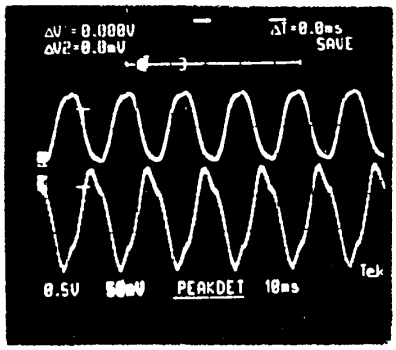

Fig. 12. Motor supplied directly from sinusoidal supply (EXPER.1) for 8% unbalance in one phase. Top: Current phase C (1.608 A rms). Bottom: Current phase B (2.515 A rms). Time scale: 10 ms/div.

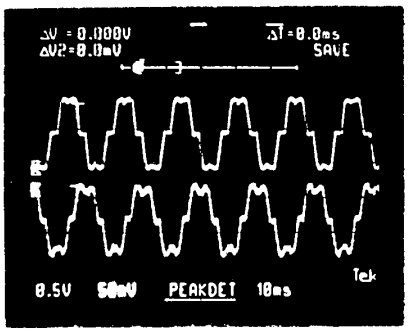

Fig. 13. Motor supplied by static starter with new controller (EXPER.2) for 8% unbalance in one phase. Top: Current phase A (1.921 A rms). Bottom: Current phase B (1.917 A rms). Time scale: 10 ms/div.

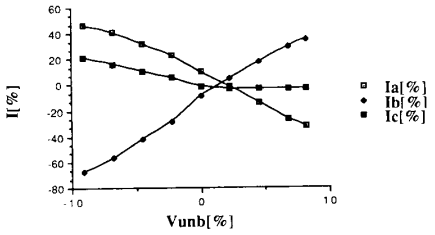

Fig. 14. Currents in each phase versus percentage of unbalanced voltage (EXPER.1) (no load condition).

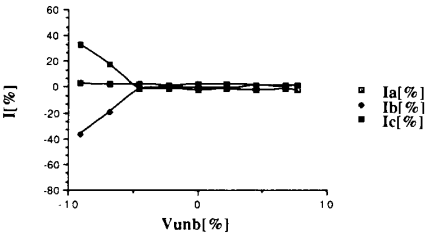

Fig. 15. Curreents in each phase versus percentage of unbalanced voltage (EXPER.2) (no load condition).

the flux level in the machine. The average current in the three phases is 1.95 A rms. Fig. 13 shows the results for EXPER.2 for the same conditions. The distinct advantages of operation of solid-state voltage controller is clearly shown.

In the next series of tests the motor was subjected to a different percentage of voltage unbalance from $+10\%$ to -10%, and the motor was operated under both no-load and full-load conditions. In Fig. 14 the experimental results for EXPER.1 for the no-load case are shown. On the vertical axis, the currents in the three phases are expressed as the percentage of the average current. Fig. 15 shows the results for the EXPER.2 for the same conditions. The results indicate the excellent capability of the new controller for balancing motor currents when subjected to an unbalanced supply. Note, however, that for a negative percentage of unbalanced voltage supply greater than -5%, the new controller loses control capability because the balancing current loops outputs $\Delta\alpha_a$, $\Delta\alpha_b$, $\Delta\alpha_c$ have the constraint that $(\alpha_o + \Delta\alpha_i) > 0$, with $i = a, b, c$. To increase the controllability range (maximum negative $\Delta\alpha_i$), it is clear that the supply voltage must be increased. Thus to obtain rated

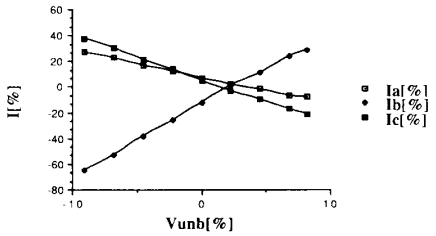

Fig. 16. Currents in each phase versus percentage of unbalanced voltage (EXPER.1) (full load condition).

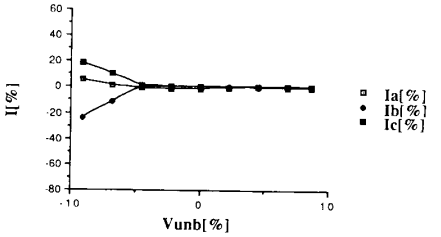

Fig. 17. Currents in each phase versus percentage of unbalanced voltage (EXPER.2) (full load condition).

TABLE I
SUMMARY OF SEVERAL PERFORMANCE PARAMETERS FOR WORST CASE CONDITION WHEN THE SUPPLY VOLTAGE UNBALANCE VARIES FROM -7.5% TO $+7.5\%$ AND THE MOTOR OPERATES UNLOADED

	EXPER.1	EXPER.2
Maximum positive unbalance of current (%)	+40.0	+2.0
Maximum negative unbalance of current (%)	−60.0	−2.5
Maximum ratio negative over positive current of voltage (%)	6.0	3.0
Maximum ratio negative over positive sequence of voltage (%)	70.0	4.0
Minimum ratio negative over positive sequence impedance (%)	8.0	7.0

voltage at the machine terminals α_o (always positive) must be increased, and hence the controllability range increases. However, this increase in α_o also increases the motor losses so that a practical limit is reached wherein the harmonic losses become intolerable. This study has established, however, that $a \pm 10\%$ unbalanced can be corrected with very modest additional motor harmonic losses.

In Figs. 16 and 17 the results related to EXPER.1 and EXPER.2 during full load are shown. Note in Fig. 17 that the controller again loses control capability at around -5% of unbalanced voltage, but the three currents continue to remain more balanced than for the no load case.

Table I summarizes the results of the previous tests together with some additional data. Of particular interest are the figures reported in lines (3) and (4) of Table I. In the case of EXPER.1 with just a few percent of negative sequence voltage, the related ratio between the negative and the positive sequence current is 45%. In the case of EXPER.2 the ratio between the negative and positive sequence of current is only 1.4%. In Fig. 18 the efficiency versus the percentage of unbalanced voltage for EXPER.1 is shown. The results are clearly encouraging. The efficiency is almost constant over the en-

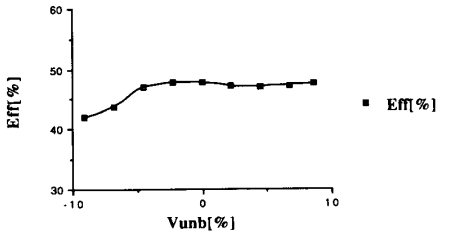

Fig. 18. Efficiency versus percentage of unbalanced voltage (EXPER.2) for full load condition.

TABLE II
CURRENT DISTORTION FACTOR FOR NO LOAD AND FULL LOAD AT THREE DIFFERENT UNBALANCED VOLTAGE CONDITIONS

	95% V rated DF (%)	100% V rated DF (%)	108% V rated DF (%)
EXPER.1			
No load	11.0	2.4	15.1
Full load	10.5	1.5	13.0
EXPER.2			
No load	21.3	19.8	23.9
Full load	20.9	18.9	23.1

tire range of control. Out of the control range, the efficiency decreases in significantly.

Finally, Table II shows the distortion factors (DF's) for the motor current over the range of unbalanced voltage -5% to $+10\%$ for the EXPER.1 and EXPER.2 for the no-load and full-load conditions. The distortion factor for the case of unbalanced supply is defined here as

$$\mathrm{DF} = \frac{1}{3} \sum_{k=a,b,c} I_k \tag{9}$$

where

$$I_k = \frac{\sqrt{\sum_{n=2}^{\infty} I_{kn}^2}}{I_{k1}}. \tag{10}$$

As expected, when the supply voltages are balanced, the distortion factors in the case of a back-to-back thyristor supply is relatively poor due to presence of harmonics. On the other hand, with an unbalanced condition the distortion factors for the sinusoidal supply and the back-to-back thyristor supply are much closer. Moreover, the "distortion factor" is quite consistent over the entire control range in the case of converter supply, whereas for the case of sinusoidal supply the harmonic content is remarkably variable.

CONCLUSION

A powerful digital controller for correcting phase unbalance in an induction motor supply has been presented by utilizing unsymmetrical control of a static starter. The major advantage of the approach that has been implemented results from the relatively inexpensive and straightforward use of power electronic components. In cases where the static starter is needed for starting purposes, the phase balance feature could be incorporated for a modest cost. If the static starter is not installed, the approach could still prove desirable in chronic situations due to the rapid response and extreme flexibility of the approach. In such situations the added benefits of soft starting and efficiency improvement under light load could be attractive. The approach should prove particularly useful in difficult industrial applications where rapidly changing unbalance conditions preclude the use of fixed capacitor banks or other conventional compensation schemes.

REFERENCES

[1] E. Muljadi, R. Schiferl, and T. A. Lipo, "Induction machine phase balancing by unsymmetrical thyristor voltage control," *IEEE Trans. Ind. Appl.*, vol. IA-21, pp. 610-616, May/June 1985.

[2] J. Oyama, F. Profumo, E. Muljadi, and T. A. Lipo, "A digital voltage controller for reducing induction motor phase unbalance," in *Conf. Rec. ICEM* 99, Pisa, Italy, Sept. 1988.

[3] F. M. Khater and D. W. Novotny, "An equivalent circuit model for phase back voltage control of ac machines," in *Proc. IEEE/IAS Annu. Meeting*, Toronto, ON, Canada, 1985, pp. 798-804.

[4] J. Oyama, S. Toba, T. Higuchi, and E. Yamada, "The characteristics of half-wave rectified brushless synchronous motor," in *Conf. Rec. BICEM'87, Beijing*, China, Aug. 1987, pp. 654-657.

[5] F. J. Nola, "Power factor control for ac induction motor," U.S. Patent 4 052 648, Oct. 4, 1977.

[6] R. F. Woll, "Effect of unbalanced voltage on the operation of polyphase induction motors," *IEEE Trans. Ind. Appl.*, vol. IA-11, no. 1, pp. 38-42, Jan./Feb. 1977.

[7] N. L. Schmitz and M. M. Berndt, "Derating polyphase induction motors operated with unbalanced line voltages," *IEEE Trans. Power App. Syst.*, no. 64, Feb. 1963, pp. 680-686.

[8] J. E. Williams, "Operation of 3 phase induction motors on unbalanced voltages," *AIEE Trans. Power App. Syst.*, vol. 73, pt. III, pp. 125-133, Apr. 1954.

[9] T. M. Rowan and T. A. Lipo, "A quantitative analysis of induction motor performance by SCR voltage control," *IEEE Trans. Ind. Appl.*, vol. IA-19, pp. 545-553, July/Aug. 1983.

[10] T. A. Lipo, "The analysis of induction motor voltage control by symmetrical triggered thyristors," *IEEE Trans. Power App. Syst.*, vol. PAS-90, no. 2, pp. 515-525, Mar./Apr. 1971.

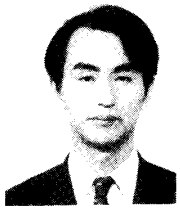

Jun Oyama (M'88) was born in Kumamoto, Japan, on March 21, 1942. He received the B.S., M.S., and Ph.D. degrees from Kyushyu University, in 1964 and 1966, and 1971, respectively.

He was a Visiting Scholar at the University of Wisconsin—Madison from June 1987 to March 1988. He is currently a Professor in the Department of Electrical Engineering and Computer Science at Nagasaki University. His principal research interests involve variable speed drives, position control drives, new type ac motors, static converters, and digital control applications.

Dr. Oyama is a member of the Institute of Electrical Engineers of Japan.

Francesco Profumo (M'88) was born in Savona, Italy, in 1953. He received the 'laurea' (with honors) in electrical engineering from the Politecnico di Torino, Italy, in 1977.

From 1978 to 1984 he worked as an R&D Engineer for the Ansaldo Group. He then joined the Department of Electrical Engineering of the Politecnico di Torino, where he is now an Assistant Professor of Electrical Machinery. He was a Visiting Professor in the Department of Electrical and Computer Engineering of the University of Wisconsin—Madison in 1986–1988. His fields of interest are power electronics conversion, integrated electronic/electromechanical design, high response speed servo drives.

Dr. Profumo is a Registered Professional Engineer in Italy and a member of IAS and PES.

Eduard Muljadi (M'80) received the E.E. degree from Surabaya Institute of Technology, Indonesia, and the M.S. and Ph.D. degrees from the University of Wisconsin, Madison in 1981, 1984, and 1987 respectively.

In 1988 he joined the Department of Electrical Engineering at California State University, Fresno, CA as a faculty member. His current teaching and research interests are in the fields of power systems, electric machine drives and power electronics.

Thomas A. Lipo (M'64-SM'71-F'87) is a native of Milwaukee, WI. He received the B.E.E. and M.S.E.E. degrees from Marquette University, Milwaukee, WI and the Ph.D. degree in electrical engineering from the University of Wisconsin, Madison, in 1962, 1964, and 1968, respectively.

Upon graduation he was a National Research Council Postdoctoral Fellow at the University of Manchester Institute of Science and Technology, Manchester, England, during the period 1968–1969. From 1969 to 1979 he was an Electrical Engineer in the Power Electronics Laboratory of Corporate Research and Development of the General Electric Company, Schenectady, NY. He became Professor of Electrical Engineering at Purdue University in 1979 and in 1981 he joined the University of Wisconsin in the same capacity.

Dr. Lipo has maintained a deep research interest in power electronics and ac drives for over 25 years. He has received 11 IEEE prize paper awards for his work including co-recipient of the Best Paper Award in the IEEE Industry Applications Society Transactions for the year 1984. In 1986 he received the Outstanding Achievement Award from the IEEE Industry Applications Society for his contributions to the field of ac drives.